OPTICAL AND QUANTUM EFFICIENCY ANALYSIS OF (Ag,Cu)(In,Ga)Se_2 ABSORBER LAYERS

Jonathan Boyle[1,2], Gregory Hanket[1], and William Shafarman[1,2]

1. Institute of Energy Conversion, University of Delaware, Newark, DE 19716
2. Department of Materials Science and Engineering, University of Delaware, Newark, DE 19716

ABSTRACT

(Ag,Cu)(In,Ga)Se_2 thin films have been deposited by elemental co-evaporation over a wide range of compositions and their optical properties characterized by transmission and reflection measurements and by relative shift analysis of quantum efficiency device measurements. The optical bandgaps were determined by performing linear fits of $(\alpha h\nu)^2$ vs. hv, and the quantum efficiency bandgaps were determined by relative shift analysis of device curves with fixed Ga/(In+Ga) composition, but varying Ag/(Cu+Ag) composition. The determined experimental optical bandgap ranges of the Ga/(In+Ga) = 0.31, 0.52, and 0.82 groups, with Ag/(Cu+Ag) ranging from 0 to 1, were 1.19-1.45 eV, 1.32-1.56 eV, and 1.52-1.76 eV, respectively. The optical bowing parameter of the different Ga/(In+Ga) groups was also determined.

INTRODUCTION

One approach to increase the efficiency of Cu(In,Ga)Se_2-based modules is to increase V_{OC} by increasing the bandgap (E_g) [1]. Increasing V_{OC} will also lead to a reduction in resistive power losses [2]. An increase in V_{OC} with E_g has been well-established by alloying with Al, Ga, and/or S into the $CuInSe_2$ alloy, but in all cases, with E_g > 1.3 eV, the efficiency decreases and V_{OC} saturates at 800 – 850 mV [2]. The inclusion of Ag into the Cu(In,Ga)Se_2 alloy to form (Ag,Cu)(In,Ga)Se_2 is being investigated as a means to increase V_{OC} and improve the performance of wide bandgap devices by lowering the melting point temperature of the material, potentially leading to lower defect densities [3]. Improved wide bandgap solar cells may also enable their application as a top cell in a tandem cell device.

Previous studies by Avon, et al. [4] of ampoule-synthesized-ingot (Ag,Cu)(In,Ga)Se_2 have determined the optical bandgap and optical bowing parameter for limited compositional ranges. This work expands upon this in determining the bandgaps and the bowing parameters for a wider range of compositions of (Ag,Cu)(In,Ga)Se_2 thin films. Supplementary work by Avon, et al. [5] on the same (Ag,Cu)(In,Ga)Se_2 ampoule-synthesized-ingot-based samples also reported a chalcopyrite-chalcopyrite immiscibility gap for certain bulk compositions. X-ray diffraction (XRD) studies of the thin films studied here showed a single phase throughout the alloy compositional system. Details on the XRD studies along with device results and analysis are reported at this conference [6].

In this work, we characterized the optical properties of (Ag,Cu)(In,Ga)Se_2 thin films deposited by elemental co-evaporation with systematic changes in the relative Ag/(Cu+Ag) and Ga/(In+Ga) compositions. Changes in bandgap determined by optical transmission and reflection measurements on thin films on bare glass and from quantum efficiency (QE) curves of devices are compared.

EXPERIMENTAL

The (Ag,Cu)(In,Ga)Se_2 samples were deposited using elemental co-evaporation from Knudsen sources onto Mo-coated soda lime glass (SLG) and bare soda lime glass substrates. Elemental fluxes were kept constant for a 60 minute deposition, with the substrate temperature held at 550°C. The resulting films were 2 µm thick. The samples had a range of compositions spanning $w \equiv$ Ag/(Cu+Ag) from 0 to 1, and $x \equiv$ Ga/(In+Ga) from 0.31 to 1. Target w/x = (Cu+Ag)/(In+Ga) compositions were within the range of 0.8 to 0.9. Compositions were determined by energy dispersive x-ray spectroscopy (EDS). A typical quantum efficiency absolute error for composition determined from the EDS measurements for a Cu(In,Ga)Se_2 control sample gave $x = 0.31 \pm 0.04$ ($w = 0$), which gives ± 0.02 eV for the bandgap analysis.

The samples on bare soda lime glass substrates were analyzed using a Perkin-Elmer UV/Vis/NIR spectrophotometer equipped with an integrating sphere. Total transmission (T) and reflection (R) data were obtained from 500-2500 nm at 1 nm intervals. The T and R data was smoothed with a 5 point box smooth. Mo films were deposited by dc sputtering and the Mo-coated soda lime glass substrate samples were fabricated into solar cell devices with the structure: SLG/Mo/(Ag,Cu)(In,Ga)Se_2/CdS/ZnO/ITO/Ni:Al grids. The CdS was deposited by chemical bath deposition, the ZnO and ITO were deposited by RF sputtering, and the Ni:Al grids were electron-beam evaporated. Quantum efficiency results were obtained under white light bias and as a function of voltage.

RESULTS

The normalized transmission [T/(1-R)] curves of a set of films with $x = 0.31 \pm 0.02$ and w spanning 0 to 1 are shown in Figure 1. The increasing bandgap with

increasing *w* is seen in the shift of the transmission curves to lower wavelengths or higher energies.

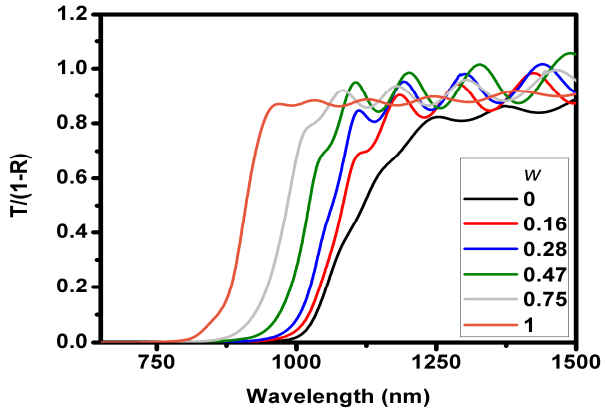

Figure 1. Normalized transmission T/(1-R) for films with *x* = 0.31 and varying *w*.

It can also be seen from the transmission spectra in the sub-bandgap energy range, that the control Cu(In,Ga)Se_2 (*w* = 0) sample has greater sub-band gap absorption (lower transmission) than the (Ag,Cu)(In,Ga)Se_2 samples [7]. This suggests that the (Ag,Cu)(In,Ga)Se_2 films may have a lower density of defects than the control Cu(In,Ga)Se_2 (*w* = 0) sample [7]. Transient photospectroscopy measurements on similar samples showed sharper optical bandtails which were similarly attributed to higher quality material [8]. The high transmission in the (Ag,Cu)(In,Ga)Se_2 films would be beneficial for application to the top cell in a tandem structure.

The optical bandgap was determined from the transmission and reflection data using a standard analytical procedure [9]. The absorption coefficient (α) was determined using Equation (1):[10]

$$\alpha(\lambda, R, T) = \left(\frac{1}{d}\right)\ln\left[\frac{(1-R)^2}{T}\right] \qquad (1)$$

where d is the sample thickness in cm and λ is the incident wavelength. The bandgap was determined by plotting $(\alpha h\nu)^2$ vs. $h\nu$ and performing a linear fit of the data. This assumes that the fundamental optical transition is due to a direct allowed transition in all cases [9]. Sample curves are shown in Figure 2 for two *x* = 0.3 samples (*w* = 0 and 1).

As can be seen in Figure 2, the samples have a linear region, which is fit to determine E_g. At higher energies, the increased slope of the Cu(In,Ga)Se_2 control is attributed to the non-degenerate valence band splitting of chalcopyrite materials [9]. It is not known at this time whether the differences in curve shape and slope of the two samples can be attributed to changes in band splitting, due to crystal-field and spin-orbit splitting, a reduction in defects, a combination of both, or other effects.

The results of the linear fits of Figure 2 are presented in Table I, and the values of E_g similarly determined for *x* = 0.31, 0.52, and 0.82 are listed in Table II. With wider bandgap films that have greater *w*, the linear region becomes smaller and determination of E_g becomes less accurate as seen by the statistical absolute error (ΔE_g).

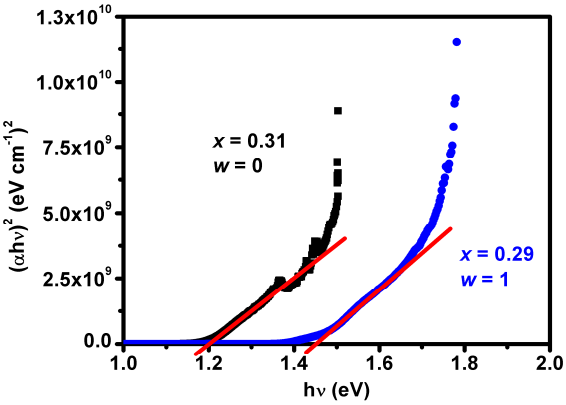

Figure 2. $(\alpha h\nu)^2$ vs. $h\nu$ for 2 films with x = 0.31: black) Cu(In,Ga)Se_2 control (w = 0), blue) (Ag,Cu)(In,Ga)Se_2 with w = 1. Red lines show the extended fitline to determine E_g.

Table I. Bandgaps determined from T and R measurements for samples from Figure 2 with x = 0.31. Included are the statistical absolute error (ΔEg) and coefficient of determination (r^2) of the fits.

w	E_g (eV)	ΔE_g (eV)	r^2	Number of data points for fit
0	1.19	0.01	0.9976	100
1	1.45	0.01	0.9992	75

Table II – Bandgaps estimated from T and R measurements for (Ag,Cu)(In,Ga)Se_2 thin films for x groups.

x	w	E_g (eV)	ΔE_g (eV)
0.31	0	1.19	0.01
	0.16	1.20	0.01
	0.28	1.22	0.01
	0.47	1.26	0.01
	0.75	1.34	0.01
	1	1.45	0.01
0.52	0	1.32	0.01
	0.27	1.35	0.01
	0.46	1.39	0.02
	0.76	1.47	0.02
	1	1.56	0.02
0.82	0[11]	1.52	0.01
	0.16	1.55	0.03
	0.27	1.58	0.02
	0.50	1.61	0.03
	0.76	1.63	0.04
	1	1.76	0.03

The bandgaps from Table II are shown in Figure 3. For each set of different x, the optical bowing parameter (b) was determined using Equation 2:[12]

$$E_g(A,B) = xE_g(A) + (1-x)E_g(B) - x(1-x)b \quad (2)$$

where x is the composition ratio for Ag, E_g(A,B) is the bandgap at that Ag composition, and E_g(A) and E_g(B) are the highest and lowest values of E_g in the group, respectively. The values of b are listed in Table III.

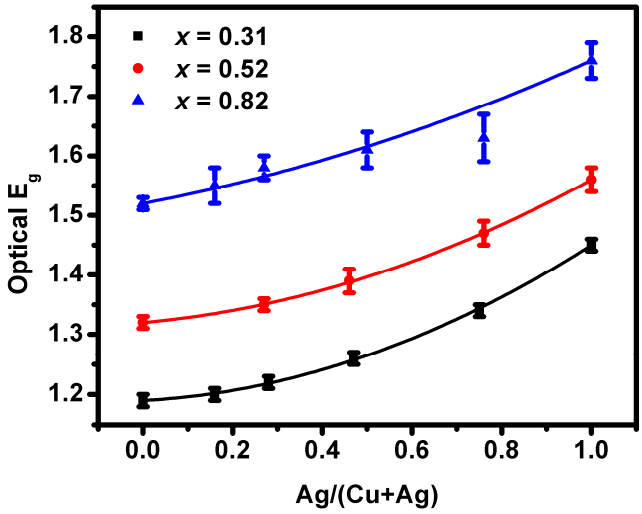

Figure 3. Optical bowing parameter fitting plots by *x* groups.

Table III – Optical bowing parameters determined from Equation 2 fitting, for *x* groups. The error for b (Δb) is the standard error ($\sigma / \sqrt{N}$).

x	b	Δb
0.31	0.20	0.02
0.52	0.17	0.01
0.82	0.10	0.05

The bandgaps from the above films, along with the results from a few additional samples are replotted in Figure 4 with fixed *w* and varying *x*. The curves show fits with Equation 2, where in this case the x parameter corresponds to the Ga composition ratio, and the resulting bowing parameters are listed in Table IV. In Figure 4 literature values were used for the *x* = 0 case [13] and the *w* = 0 case [11].

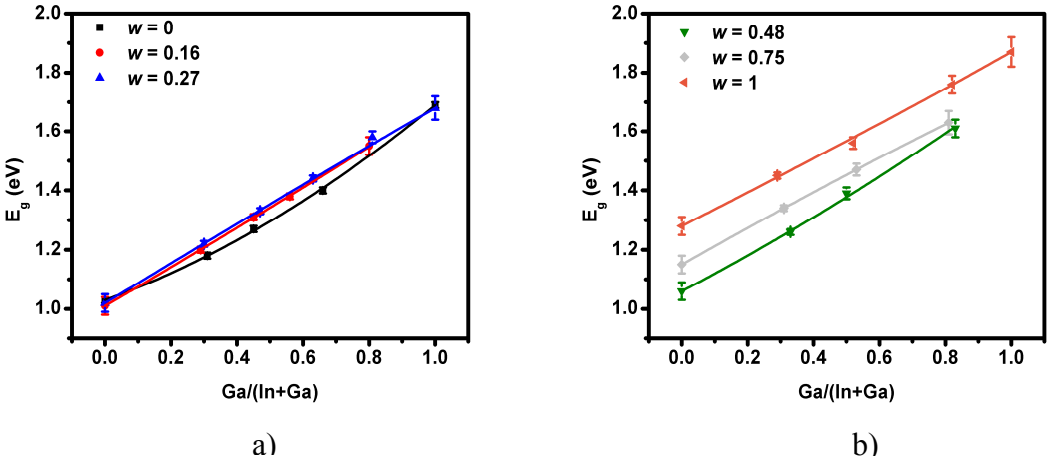

Figure 4. Bandgaps for sets of samples with fixed *w* and varying *x* and corresponding fits to determine b. a) *w* = 0-0.27 and b) *w* = 0.48-1.

Table IV – Optical bowing parameters with fixed *w* and varying *x*. Error for b (Δb) is standard error ($\sigma / \sqrt{N}$).

w	b	Δb
0	0.26	0.01
0.16	0.03	0.02
0.27	-0.01	0.01
0.48	0.11	0.05
0.75	-0.04	0.01
1	0.03	0.02

Figure 4 shows a similar result to Figure 3 in that the bandgap does not increase much with slight additions of Ag to Cu(In,Ga)Se_2. Only at *w* > 0.48 does the bandgap effectively increase. This is readily visible in Figure 4 (a) in that the *w* = 0.16 and 0.27 groups overlay each other and show only a slight increase in bandgap compared to the *w* = 0 control.

Normalized QE curves of devices using (Ag,Cu)(In,Ga)Se_2 with *x* = 0.31 are shown in Figure 5. The bandgaps of the (Ag,Cu)(In,Ga)Se_2 samples were determined by the relative shift in the long wavelength QE edge from the Cu(In,Ga)Se_2 sample at the horizontal dashed line. This line is positioned to give the value of E_g = 1.19 eV for the Cu(In,Ga)Se_2 sample, as determined from the optical analysis above and in agreement with the literature result for that composition determined using spectroscopic ellipsometery [11]. This analysis assumes there are no significant differences in current collection in the devices which would change the slope of the QE edges. The E_g results are compared to the optical results with *x* = 0.31 in Table V and the two methods yield similar results. Small differences with *w* = 0.75 and 1 may be an indication of greater uncertainty in the optical analysis.

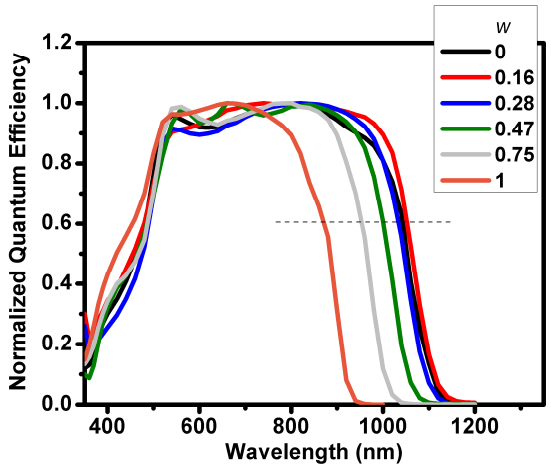

Figure 5. Normalized quantum efficiency curves for *x* = 0.31 and varying *w*. The black dashed horizontal line shows where the relative shift analysis to determine E_g was performed.

Table V. Bandgaps estimated from T and R measurements and QE results for samples with *x* = 0.31.

w	Optical E_g (eV)	Optical ΔE_g (eV)	QE E_g (eV)
0	1.19	0.01	1.19
0.16	1.20	0.01	1.18
0.28	1.22	0.01	1.20
0.47	1.26	0.01	1.24
0.75	1.34	0.01	1.30
1	1.45	0.01	1.42

The QE curves were compared for devices with *x* = 0.52 and 0.82, but are not shown. The QE curves for those *x* groups had different long-wavelength tail slopes, attributed to differences in current collection [14], which prohibited determination of E_g from the QE.

CONCLUSIONS

$(Ag,Cu)(In,Ga)Se_2$ films have been grown by elemental co-evaporation and their optical properties and bandgaps characterized by UV/Vis/NIR spectrophotometry. Low sub-band absorption of the $(Ag,Cu)(In,Ga)Se_2$ samples suggest that the samples had lower densities of defects, compared to $Cu(In,Ga)Se_2$. Bandgaps were determined by analysis of T and R measurements and the optical bowing parameters were determined for alloying with Ag/(Cu+Ag) or Ga/(In+Ga). For Ga/(In+Ga) = 0.31, the optical E_g results were compared to E_g determined by the shift in the QE edge of solar cell devices from the same deposition and gave good agreement. With higher Ga contents, the QE edges had different slopes so quantitative analysis of the shifts to determine E_g could not be completed.

ACKNOWLEDGEMENTS

The authors wish to thank Josh Cadoret, Dan Ryan, Brad Culver, John Allen, and other IEC personnel for their assistance in sample production and sample/device characterization. This material is based upon work supported by the Department of Energy under Award Number DE-FG36-08GO18019.

Disclaimer

This report was prepared as an account of work sponsored by an agency of the United States Government. Neither the United States Government nor any agency thereof, nor any of their employees, makes any warranty, express or implied, or assumes any legal liability or responsibility for the accuracy, completeness, or usefulness of any information, apparatus, product, or process disclosed, or represents that its use would not infringe privately owned rights. Reference herein to any specific commercial product, process, or service by trade name, trademark, manufacturer, or otherwise does not necessarily constitute or imply its endorsement, recommendation, or favoring by the United States Government or any agency thereof. The views and opinions of authors expressed herein do not necessarily state or reflect those of the United States Government or any agency thereof.

REFERENCES

[1] *Handbook of Photovoltaic Science and Engineering*, A. Luque and S. Hegedus, Eds., John Wiley and Sons, Inc. Hoboken, New Jersey, 2003, Chapter 3.

[2] *Handbook of Photovoltaic Science and Engineering*, A. Luque and S. Hegedus, Eds., John Wiley and Sons, Inc. Hoboken, New Jersey, 2003, Chapter 13.

[3] *Kinetics of Materials*, R.W. Balluffi, S.M. Allen, and W.C. Carter, John Wiley and Sons, Inc. Hoboken, New Jersey, 2005, Chapter 8.

[4] J. Avon, K. Yoodee, and J.C. Woolley, *Nuovo Cimento Soc. Ital. Fis., D Condensed Matter, Atomic, Molecular and Chemical Physics, Biophysics*, **2** 6 (1983) 1858-1868.

[5] J.E. Avon, K. Yoodee, and J.C. Woolley, *J. Appl. Phys.* **55** 2 (1984) 524-535.

[6] G.M. Hanket, J.H. Boyle, W.N. Shafarman, 34th IEEE PVSC, June 7-12, Philadelphia, PA, 2009, to be published.

[7] N. Kavcar, *Sol. Energy Mater. and Sol. Cells* **52** (1998) 183-195.

[8] P. Erslev, J.D. Cohen, G. Hanket, and W. Shafarman, MRS Spring Meeting, Apr. 13-17, San Francisco, CA, 2009, to be published.

[9] T. Colakoglu, M. Parlak, S. Oezder, *J. Non-Cryst. Solids* **354** (2008) 3630-3636.

[10] N. Khemiri, F.C. Akkari, M. Kanzari, B. Rezig, *Thin Solid Films* **516** (2008) 7031-7035.

[11] P.D Paulson, R.W. Birkmire, and W.N. Shafarman, *J. Appl. Phys.* **94** 2 (2003) 879-888.

[12] J.E. Bernard and A. Zunger, *Physical Rev. B.* **34** 8 (1986) 5992-5996.

[13] R. Bacewicz, J.R. Durrant, T.F. Ciszek, and S.K. Deb, *Proceedings of the 7th International Conference on Ternary and Multinary Compounds* (1987) 155-160.

[14] S.S. Hegedus and W.N. Shafarman, *Prog. Photovolt: Res. Appl.* **12** (2004) 155-176.